Antibacterial mechanism of geraniol against *Staphylococcus aureus* by targeting the cell membrane

Keshan Lin[1,2†], Jialin Dai[1†], Rui Zhang[1†], Renkun Lai[1], Peng Zhang[1], Lizhu Shen[1], Chunyang Li[1], Lin Lin[1,3], Min Dai[1,3*], Fenghui Sun[1,4*]

[1]School of Laboratory Medicine, Chengdu Medical College, Chengdu, Sichuan, China; [2]Department of Medical Laboratory, Chengdu Seventh People's Hospital (Affiliated Cancer Hospital of Chengdu Medical College), Chengdu, Sichuan, China; [3]Sichuan Provincial Engineering Laboratory for Prevention and Control Technology of Veterinary Drug Residue in Animal-origin Food, Chengdu Medical College, Chengdu, China; [4]Second Affiliated Hospital of Chengdu Medical College, China National Nuclear Corporation 416 Hospital, Chengdu, Sichuan, China

[†]These authors contributed equally to this work

[*]**Corresponding Authors:** Fenghui Sun, Second Affiliated Hospital of Chengdu Medical College, China National Nuclear Corporation 416 Hospital, Chengdu, Sichuan, China. Email: sunfenghui@cmc.edu.cn; Min Dai, Sichuan Provincial Engineering Laboratory for Prevention and Control Technology of Veterinary Drug Residue in Animal-origin Food, Chengdu Medical College, Chengdu, China. Email: daimin1015@cmc.edu.cn

Academic Editor: Saeid Jafari, Department of Food Technology, Chulalongkorn University, Bangkok

Received: 19 July 2025; Accepted: 21 April 2026; Published: 26 May 2026

ORIGINAL ARTICLE

Abstract

Geraniol exhibits strong antibacterial activity against methicillin-resistant *Staphylococcus aureus* (MRSA) in both *in vitro* and *in vivo*; yet its underlying mechanism remains incompletely understood. Our study systematically characterized the antibacterial mode of action of geraniol using flow cytometry, fluorescence spectroscopy, electron microscopy, and molecular dynamics simulations. The results showed that geraniol readily partitions into the lipid bilayer and disrupts membrane integrity, with 81.95% of cells exhibiting membrane damage at 1.380 mg/mL. Consistently, geraniol treatment increased membrane fluidity, as indicated by a reduction in fluorescence polarization from 0.410 to 0.380, and was associated with conformational alterations in membrane proteins. These membrane perturbations were accompanied by extensive downstream damage, including leakage of intracellular components, with extracellular levels increasing by 9.61-fold for DNA, 11.82-fold for RNA, and 15.92-fold for proteins. Additionally, ultrastructural analyses revealed cell wall thinning from 0.037 μm to 0.026 μm and marked DNA condensation. Collectively, these findings indicate that the MRSA cell membrane represents a primary target of geraniol, with subsequent structural damage likely resulting from severe membrane dysfunction and disruption of cellular homeostasis. This study provides mechanistic insights supporting the potential development of geraniol as a membrane-targeting antibacterial agent.

Keywords: cell wall, geraniol, membrane damage, molecular dynamics, MRSA

Introduction

Staphylococcus aureus is a clinically significant pathogen associated with a broad range of severe diseases, including skin and soft tissue infections (Hatlen & Miller, 2021), bacteremia (Tabah & Laupland, 2022), osteomyelitis (Song *et al*., 2025), and toxic shock syndrome (Mele & Madrenas, 2010). Beyond clinical settings, this organism is also a prominent cause of foodborne illness, contributing substantially to both sporadic cases and outbreaks of food poisoning (Cheung *et al*., 2021; Nunes Nascimento *et al*., 2025). In the United States alone, *S. aureus* is responsible for approximately 241,000 cases of foodborne infection annually, leading to over 1,000 hospitalizations and several fatalities (Scallan *et al*., 2011). The increasing prevalence of methicillin-resistant *S. aureus* (MRSA), particularly in meat and dairy products, has further exacerbated public health concerns, presenting an ongoing challenge to both food safety and infection control (Ning *et al*., 2023; Yu *et al*., 2023).

Chemical preservatives, such as sodium benzoate, sorbic acid, and sodium dehydroacetate, are widely employed in the food industry to inhibit microbial growth and prolong shelf life (Ekhtelat *et al*., 2020; Selim *et al*., 2022; Wu *et al*., 2025). Notwithstanding their effectiveness, increasing attention has been directed toward their potential adverse effects on human health, including gastrointestinal, respiratory, and neurological disturbances, as well as possible carcinogenic and teratogenic risks (Novais *et al*., 2022). These concerns have prompted heightened regulatory scrutiny and underscored the need for safer alternatives with improved biocompatibility and reduced toxicological burden (Mamur *et al*., 2012). In this regard, naturally derived compounds, such as geraniol, citral, and citronellal, have attracted growing interest as multifunctional food additives capable of enhancing flavor, extending shelf life, and mitigating microbial contamination (D'Souza *et al*., 2017; Olszewska *et al*., 2020; Ribeiro-Santos *et al*., 2017; Teshome *et al*., 2022).

Among these natural compounds, geraniol has garnered attention due to its broad-spectrum antibacterial activity against various pathogens, including *S. aureus* (Gu *et al*., 2022), *Acinetobacter baumannii* (Kim *et al*., 2022), *Listeria monocytogenes* (Friedman *et al*., 2002), *Escherichia coli* (Feng *et al*., 2022), and *Pseudomonas aeruginosa* (Li *et al*., 2023), and its potentiating effects on the efficacy of β-lactam antibiotics against MRSA (Kannappan *et al*., 2019). In addition to its antimicrobial properties, geraniol exerts diverse bioactive effects, including anti-inflammatory (Jayachandran *et al*., 2015), anticancer (Silva *et al*., 2022), antioxidant (Pavan *et al*., 2018), hepatoprotective (F El Azab *et al*., 2020), and neuroprotective activities (Bagheri *et al*., 2022). Together with its favorable safety profile, these features highlight its considerable potential for food preservation and therapeutic applications.

Recent investigations into the antibacterial mechanism of geraniol have largely focused on damage to the bacterial cell envelope, particularly the cell membrane (Murbach Teles Andrade *et al*., 2016; Singh & Katoch, 2020). Ultrastructural studies have shown that geraniol induces pronounced morphological injury in multiple bacterial species, including MRSA, with characteristic features such as membrane deformation and cell wall disruption (Guimarães *et al*., 2019; Murbach Teles Andrade *et al*., 2016). However, current evidence is predominantly derived from endpoint morphological observations and lacks continuous, time-resolved analysis of the damage process. Quantitative characterization of critical membrane-associated functions, including membrane integrity, membrane fluidity, and membrane protein alterations, has also remained limited. More importantly, the temporal sequence of cellular events following geraniol exposure, specifically the distinction between membrane disruption as an initiating event and as a secondary consequence of general cellular deterioration, has not been systematically established. Furthermore, the causal relationship between membrane damage and downstream structural alterations, such as cell wall thinning and DNA condensation, remains poorly defined.

This study applied an integrated, multidisciplinary approach to systematically define the antibacterial mechanism of geraniol against *S. aureus*. Dynamic changes in key membrane functional properties were quantitatively assessed following geraniol exposure, together with continuous evaluation of cell surface morphology, subcellular organization, and ultrastructural alterations. Molecular dynamics simulations were further conducted to characterize the interaction between geraniol and the bacterial lipid bilayer. Collectively, these analyses provided a more robust and quantitatively supported mechanistic framework for the antibacterial action of geraniol and establish a theoretical basis for the further development of this naturally derived compound as a membrane-targeting antibacterial agent.

Materials and Methods

Strains and chemicals

Staphylococcus aureus ATCC 43300 was obtained from the American Type Culture Collection (Manassas, VA, USA) and stored at −80°C. The bacteria were plated on nutrient agar (Aoboxing, Beijing, China) and incubated at 37°C overnight. Mueller–Hinton agar (MHA), Tryptone soy broth (TSB), and Mueller–Hinton II broth (MHB II)

were purchased from Beijing Solarbio Technology Co., Ltd. (Solarbio, Beijing, China). Geraniol (CAS: 106-24-1, purity ≥ 98%) and glutaraldehyde (CAS: 111-30-8) were purchased from Sigma-Aldrich (St. Louis, MO, USA). Nile Red (CAS: 7385-67-3), Hoechst 33342 (CAS: 23491-52-3), 1,6-diphenyl-1,3,5-hexatriene (DPH, CAS: 1720-32-7), and potassium iodide (KI, CAS: 7681-11-0) were obtained from Thermo Fisher Scientific (Waltham, MA, USA).

Growth curve assay

The growth curve assay was performed according to a previously described method (Huo *et al*., 2022), with slight modifications. Briefly, a single colony of *S. aureus* was suspended in sterile saline and adjusted to a turbidity equivalent to a 0.5 McFarland standard. This suspension was inoculated into MHB II containing varying concentrations of geraniol in a 96-well plate. The plate was incubated at 37°C for 24 h, and the OD_{600} was measured at 1 h intervals using a multimode plate reader (Bioscreen C Pro, Oy Growth Curves Ab Ltd., Helsinki, Finland). Wells containing the bacterial suspension served as the positive control, and wells with MHB II only served as the negative control. All experiments were performed in triplicate.

Time-kill curve assay

Time-kill kinetics were evaluated in accordance with the Clinical and Laboratory Standards Institute (CLSI) guideline M26-A and previously described procedures (Wang *et al*., 2023), with minor modifications. In brief, to obtain cells in the logarithmic growth phase, diluted bacterial suspensions were incubated at 37°C with shaking at 200 rpm until the OD_{600} reached 0.60, which occurred after approximately 4 h. These cells were then exposed to geraniol at a final concentration of 1.380 mg/mL. During the subsequent 5 h of incubation at 37°C, aliquots were collected at 10, 20, 40, 90, 120, 150, 180, 210, 240, 270, and 300 min, serially diluted, and spread on MHA plates for the determination of viable counts. Untreated cells, processed in parallel, served as controls. All experiments were conducted in triplicate.

Microscope observation

Morphological and ultrastructural alterations in *S. aureus* cells following geraniol treatment were examined using scanning electron microscopy (SEM, JSM-IT700HR, JEOL Ltd., Tokyo, Japan), transmission electron microscopy (TEM, JEM-1400FLASH, JEOL Ltd., Tokyo, Japan), and super-resolution structured illumination microscopy (SR-SIM, N-SIM E, Nikon Corporation, Tokyo, Japan). Experimental procedures were conducted according to previously established protocols (Hou *et al*., 2022; Jensen *et al*., 2020; Shi *et al*., 2018). Specifically, *S. aureus* cultures adjusted to 0.5 McFarland were treated with geraniol at 0.690 mg/mL or 0.345 mg/mL, with PBS-treated cultures included as controls, for 10, 40, 90, 180, and 300 min. Cells were harvested by centrifugation at 5,000 × g for 10 min at 4°C and subsequently washed three times with PBS. For SEM and TEM analyses, cell pellets were fixed in 2.5% glutaraldehyde for 6 h. For SR-SIM analysis, samples were stained at room temperature with Nile Red for membrane visualization, WGA-488 for cell wall labeling, and Hoechst 33342 for DNA staining (Supplementary Table S1). Stained samples were mounted on agarose pads prepared with 1.2% agarose in PBS and observed using SR-SIM.

Cell volume was quantified using Fiji (v1.54f) according to published protocols (Jensen *et al*., 2020), based on the formula $V = 4/3\pi ab^2$, where a and b represent the major and minor axes, respectively. At least 50 cells were analyzed at each time point. Additionally, cell wall thickness was measured from TEM images acquired at 12,000× magnification using ImageJ software (v1.54, USA).

Molecular dynamics simulations

Molecular dynamics simulations were conducted using GROMACS (v5.1.5) (Hess *et al*., 2008). The three-dimensional structure of geraniol was obtained from PubChem (http://pubchem.ncbi.nlm.nih.gov). System construction and simulation parameters were defined according to established methodology (Kim *et al*., 2020). The bacterial membrane model consisted of a mixed lipid bilayer containing 88 neutral 1,2-dioleoyl-sn-glycero-3-phosphocholine (DOPC) lipids and 40 negatively charged 1,2-dioleoyl-sn-glycero-3-phosphoglycerol (DOPG) lipids, corresponding to an approximate 7:3 ratio, and was parameterized using Berger's lipid force field (Kim *et al*., 2018). Simulations were conducted under NPT conditions at 1 atm and 300 K, with periodic boundary conditions applied in all directions and a time step of 2 fs. Following equilibration of the solvated bilayer for 500 ns, geraniol was introduced into the aqueous phase above the membrane. After an additional 100 ns re-equilibration period, the compound was released, and the system was subjected to a 50 ns production run (Creighton *et al*., 2016).

Cell constituent assays

Leakage of intracellular and extracellular nucleic acids and proteins was quantified according to previously

established protocols (Song *et al*., 2020; Yuan *et al*., 2019). Bacterial cultures were exposed to different concentrations of geraniol for 0.5, 1, 2, 4, and 6 h. At each time point, samples were collected and centrifuged at 5,000 × g for 10 min at 4°C to separate supernatants from cell pellets. The supernatants were collected before sonication for the assessment of geraniol-induced leakage of extracellular components. Cell pellets were washed, resuspended in PBS, and subjected to ultrasonic disruption using a VCX750 sonicator (Sonics, Newtown, CT, USA). The resulting lysates were centrifuged at 5,000 × g for 10 min at 4°C to obtain intracellular fractions. Nucleic acid concentrations in both extracellular and intracellular fractions were quantified using a TGem Pro spectrophotometer (Tiangen Biotech, Beijing, China), whereas protein concentrations were determined using a Bradford Assay Kit (Solarbio, Beijing, China). Untreated samples collected at corresponding time points served as controls. All experiments were conducted in triplicate.

Flow cytometry analysis

Bacterial membrane integrity was assessed using a LIVE/DEAD® BacLight™ Bacterial Viability Kit (Invitrogen, Thermo Fisher Scientific, USA) according to a protocol adapted from previous research (Bai *et al*., 2015). In brief, exponential *S. aureus* cells were harvested by centrifugation at 5,000 × g for 10 min at 4°C, washed, and resuspended in 0.85% sterile saline to a density of 1×10^9 CFU/mL. The bacterial suspension was incubated with geraniol at 37°C for 30 min. After treatment, cells were washed and diluted to 1×10^6 CFU/mL with 0.85% saline. The suspension was stained with a mixture of 10 μM SYTO9 and 60 μM propidium iodide (PI) in the dark at room temperature for 15 min. Stained cells were analyzed using an ACEA NovoCyte flow cytometer (Agilent Technologies, San Diego, CA, USA). Fluorescence signals for SYTO9 and PI were collected at 525 nm and 620 nm, respectively, with 50,000 events recorded per sample. Untreated cells and cells treated with 70% isopropyl alcohol served as negative and positive controls, respectively.

Membrane fluidity analysis

Cell membrane fluidity was determined by measuring fluorescence polarization with the hydrophobic probe 1,6-diphenyl-1,3,5-hexatriene (DPH), following a previously described method (Royce *et al*., 2013). Briefly, *S. aureus* cells (OD_{600} = 0.6) were treated with geraniol at 0.690 mg/mL or 0.345 mg/mL and incubated at 37°C for 1 h. The cells were then harvested, washed twice in PBS (pH 7.0), adjusted to 0.5 McFarland, and incubated with 1 μM DPH (D20800, Sigma-Aldrich) at 37°C for 30 min. Fluorescence polarization was immediately recorded on a FlexStation 3 multifunctional microplate reader (Molecular Devices, USA), with excitation and emission wavelengths set at 360 nm and 430 nm, respectively, employing slit widths of 5.0/5.0 nm. Fluorescence polarization was calculated as follows:

$$P = (Ivv - IvhG) / (Ivv + IvhG)$$

where P is the fluorescence polarization, G is the instrument grating factor, Ivh is the intensity of the horizontally emitted beam, and Ivv is the intensity of the vertically emitted beam.

Fluorescence analysis of membrane proteins

Fluorescence emission spectra of membrane proteins were analyzed according to previously reported methods (Wei *et al*., 2021; Wu *et al*., 2016). Cells in the logarithmic growth phase were washed with 0.85% saline, resuspended, and adjusted to 0.5 McFarland. The bacterial suspension was then exposed to different concentrations of geraniol or KI at 25°C for 1 h. Emission spectra were recorded using the same multifunctional microplate reader described above, with the excitation wavelength fixed at 258 nm and the emission wavelengths scanned from 280 nm to 400 nm.

Statistical analysis

All biological experiments were performed in triplicate. Data are presented as mean ± standard deviation (SD). Statistical comparisons were conducted using one-way analysis of variance (ANOVA) in GraphPad Prism v8.0. A p-value of less than 0.05 was deemed statistically significant. Significance levels are indicated by $^{*}p \le 0.05$, $^{**}p \le 0.01$, $^{***}p \le 0.001$, and $^{****}p \le 0.0001$.

Results

Antibacterial activity of geraniol against *S. aureus*

Our previous study demonstrated strong antibacterial activity of geraniol against multiple *S. aureus* strains, including ATCC 43300 (Sun *et al*., 2018), which served as the reference strain in the present study. Against this strain, the minimum inhibitory concentration (MIC) and minimum bactericidal concentration (MBC) of geraniol were 0.690 mg/mL and 1.380 mg/mL, respectively. Antibacterial efficacy was further evaluated by monitoring growth dynamics across a concentration gradient of geraniol. As shown in Figure 1, treatment with 0.173 mg/mL produced no significant change in bacterial growth

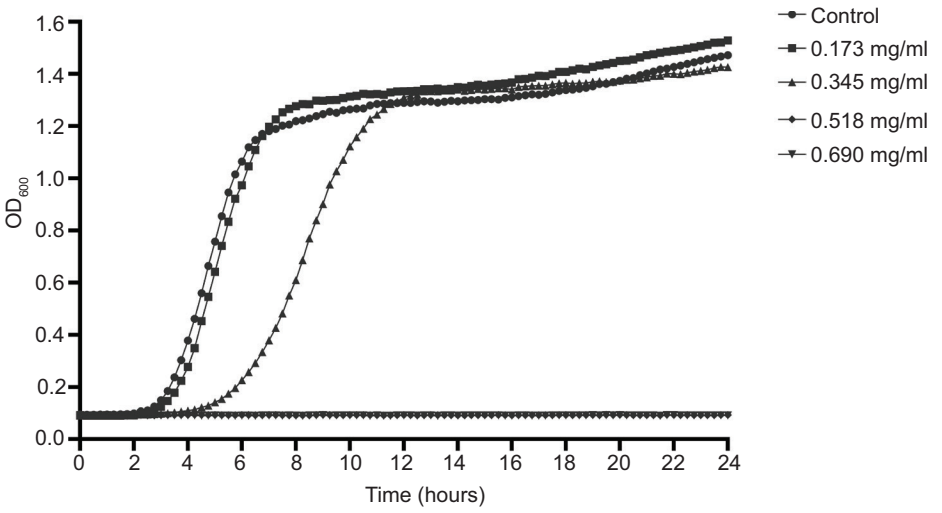

Figure 1. Growth curves of *S. aureus* ATCC 43300 cultured in MHB II containing different concentrations of geraniol. Values are presented as means from three independent experiments.

relative to the control. In contrast, 0.345 mg/mL markedly suppressed proliferation and prolonged the lag phase by 2 h, indicating a clear delay in bacterial growth. Further increases in concentration to 0.518 mg/mL and 0.690 mg/mL completely abolished detectable growth of *S. aureus*. Collectively, these data demonstrated a pronounced concentration-dependent inhibitory effect of geraniol against MRSA.

Bactericidal activity of geraniol

The bactericidal efficacy of geraniol was further evaluated through time-kill curve assays. As shown in Figure 2, in the untreated control group, the bacterial count remained stable at approximately 8.38 $\log_{10}$ CFU/mL. However, upon exposure to 1.380 mg/mL geraniol, viable cell counts began to decline rapidly, dropping to 7.34 $\log_{10}$ CFU/mL within 10 min. The count further decreased to 5.10 $\log_{10}$ CFU/mL after 40 min and reached 3.10 $\log_{10}$ CFU/mL after 2 h. These findings indicate that geraniol exerts bactericidal activity and rapidly reduces viable *S. aureus* counts.

Effects of geraniol on bacterial morphological changes revealed by SEM

To further evaluate the morphological effects of geraniol on *S. aureus* cells, SEM was performed on cells exposed to 0.690 mg/mL and 0.345 mg/mL geraniol for 10, 40, 90, 180, and 300 min. As shown in Figure 3A, untreated cells displayed a typical smooth surface and normal morphology. In contrast, after 10 min of geraniol treatment, *S. aureus* cells retained an overall smooth surface, but early wrinkles and shallow surface depressions became apparent, with shrinkage increasing in a concentration- and time-dependent manner (Figure 3B-C). After 40 min of exposure to 0.690 mg/mL geraniol, most cells exhibited significant dents or collapsed structures (Figure 3C-2). Furthermore, extensive cell lysis was observed after 90 min of treatment with 0.690 mg/mL geraniol and 300 min of treatment with 0.345 mg/mL geraniol (Figure 3C-3 and 3B-5). These observations suggest that geraniol induces surface shrinkage within the first 10 min, followed by progressive cell rupture, indicating that membrane damage and leakage of cellular contents may be central to the antibacterial activity of geraniol against *S. aureus*.

Effects of geraniol on bacterial morphological changes revealed by SR-SIM

SR-SIM imaging was conducted to characterize the structural effects of geraniol on *S. aureus*, with WGA-488 staining the cell wall green, Nile Red labeling the membrane red, and Hoechst 33342 staining DNA blue. As shown in Figure 4A, untreated cells exhibited smooth cell walls and membranes and uniformly distributed cytoplasmic DNA. Following 10 min of geraniol treatment, intense fluorescence signals appeared adjacent to the inner cell membrane, and cells became progressively smaller with increasing exposure time, suggesting cell membrane invagination. After 300 min (Figure 5), the mean cell volumes were reduced to 0.750 ± 0.20 μm^3 in the 0.345 mg/mL group and 0.530 ± 0.12 μm^3 in the 0.690 mg/mL group, both significantly smaller than the mean cell volume in the control group (0.850 ± 0.23 μm^3).

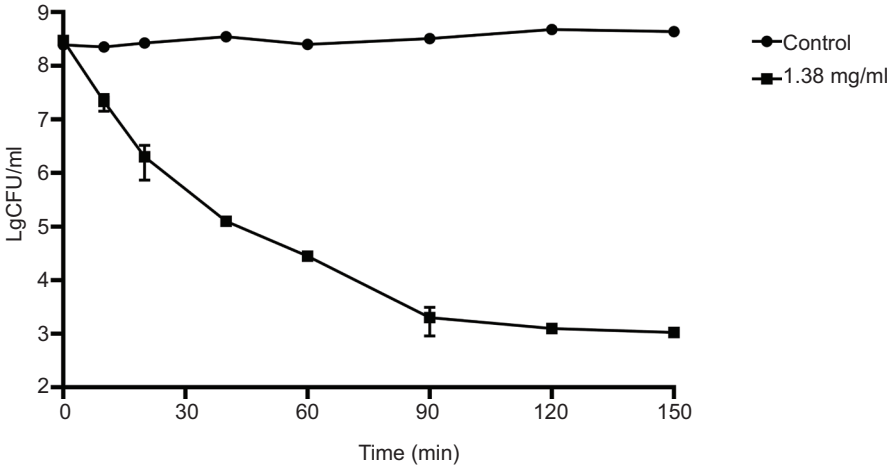

Figure 2. Time-kill curves of geraniol against *S. aureus* ATCC 43300. Values are presented as means ± standard deviation (SD) from six independent experiments.

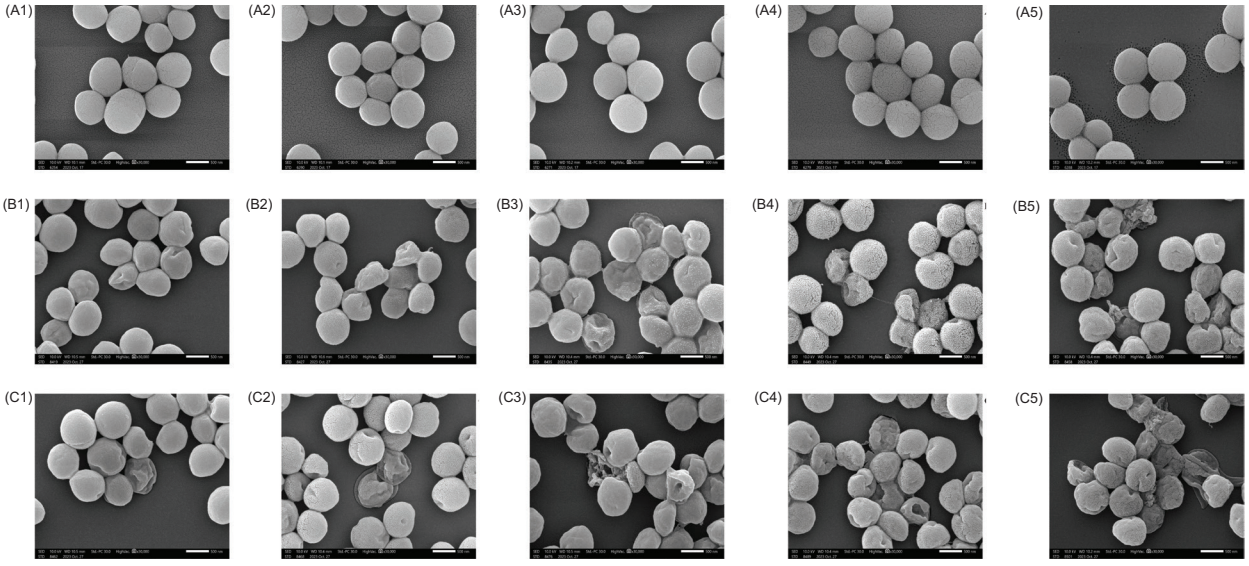

Figure 3. SEM images of *S. aureus* at 30,000× magnification. Untreated cells (A), cells treated with 0.345 mg/mL geraniol (B), and cells treated with 0.690 mg/mL geraniol (C). Panels A1, B1, and C1 correspond to 10 min; A2, B2, and C2 correspond to 40 min; A3, B3, and C3 correspond to 90 min; A4, B4, and C4 correspond to 180 min, and A5, B5, and C5 correspond to 300 min. Scale bars, 500 nm.

These findings suggest that geraniol is associated with cell membrane invagination and a reduction in *S. aureus* cell volume over time.

In addition, the fluorescence signal from the cell wall decreased or dissipated following treatment, suggesting that geraniol induces cell wall alterations, such as thinning and rupture. Notably, DNA condensation was observed after 10 min of treatment with 0.690 mg/mL geraniol (Figure 4C, 10 min).

Effects of geraniol on bacterial morphological changes revealed by TEM

TEM was used to further define ultrastructural damage in *S. aureus* following geraniol exposure. As shown in Figure 6A, untreated cells preserved normal morphology throughout the observation period, with clearly delineated cell walls, intact membrane architecture, and evenly distributed cytoplasmic contents. In contrast, geraniol-treated cells showed early

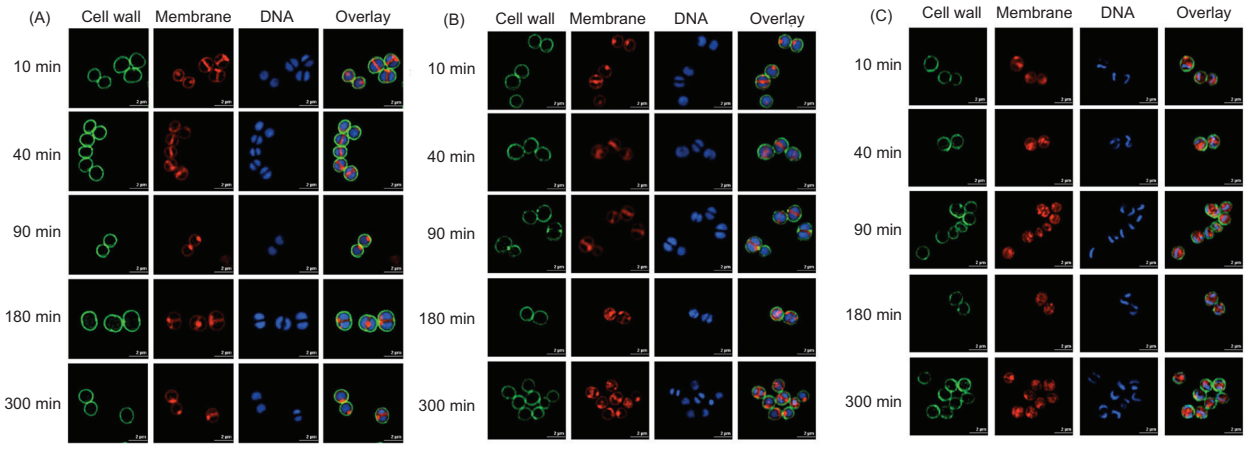

Figure 4. SR-SIM images of *S. aureus* at 512 × 512 pixel resolution. Untreated cells (A), cells treated with 0.345 mg/mL geraniol (B), and cells treated with 0.690 mg/mL geraniol (C). Scale bars, 2 µm.

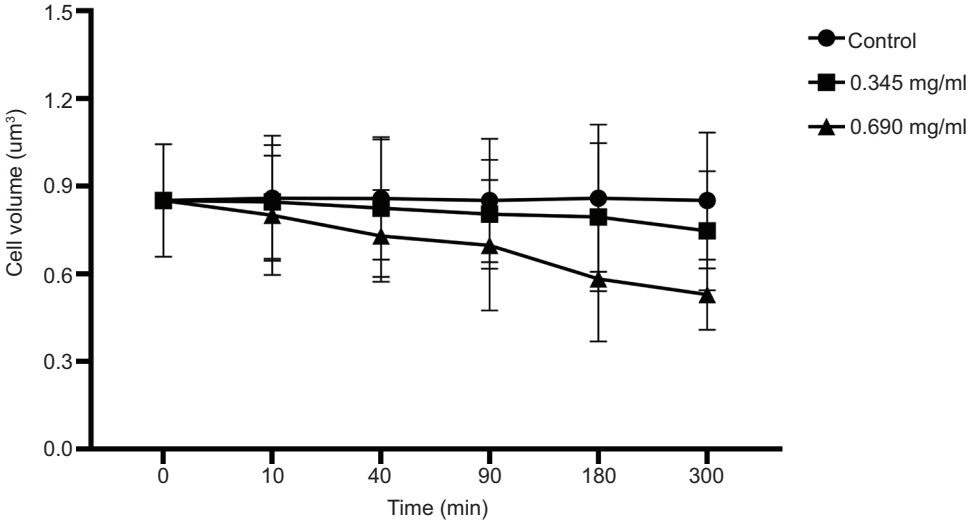

Figure 5. Effects of geraniol on cell volume of *S. aureus*. At least 50 cells were analyzed at each time point. Error bars represent SD.

ultrastructural abnormalities within 10 min, most notably detachment between the cell wall and the cell membrane (Figures 6B-1 and 6C-1). With continued exposure, cytoplasmic electron density progressively declined and became clearly reduced by 40 min (Figures 6B-2 and 6C-2). By 90 min, severe structural injury was evident, including rupture of the cell wall and pronounced membrane disruption (Figures 6B-3 and 6C-3).

Quantitative assessment of cellular integrity based on TEM observations (Table 1) further supported these morphological findings. The control group maintained 100% normal cells at all examined time points, whereas geraniol treatment produced a progressive increase in the proportion of damaged cells in both a time- and concentration-dependent manner. At 10 min, damaged cells represented 1% and 3% of the populations exposed to 0.345 mg/mL and 0.690 mg/mL geraniol, respectively. By 300 min, these values increased to 26% and 40%. These data demonstrate a continuous loss of cellular integrity during geraniol treatment and the progressive destabilization of *S. aureus* ultrastructure over time.

Cell wall thickness measurements revealed significant structural thinning after geraniol treatment. As shown in Figure 7, treatment with 0.690 mg/mL geraniol reduced

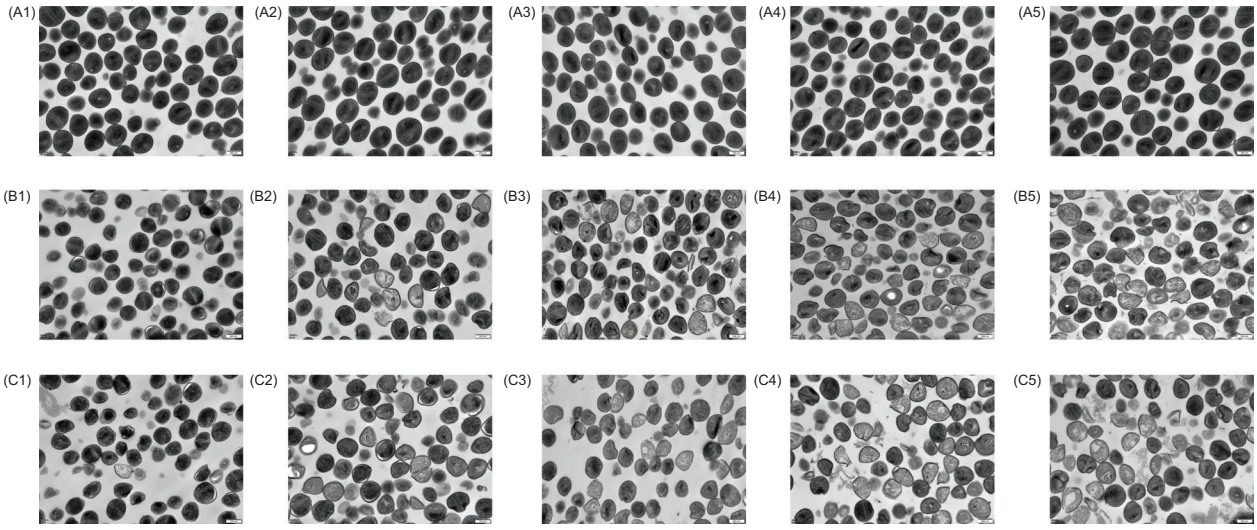

Figure 6. TEM images of *S. aureus* at 25,000× magnification. Untreated cells (A), cells treated with 0.345 mg/mL geraniol (B), and cells treated with 0.690 mg/mL geraniol (C). Panels A1, B1, and C1 correspond to 10 min; A2, B2, and C2 correspond to 40 min; A3, B3, and C3 correspond to 90 min; A4, B4, and C4 correspond to 180 min, and A5, B5, and C5 correspond to 300 min. Scale bars, 500 nm.

Table 1. Changes in cell lysis rate of *S. aureus* after treatment with geraniol (*n* = 100).

Time (min)	0.345 mg/mL geraniol		0.69 mg/mL geraniol	
	Damaged cells	Normal cells	Damaged cells	Normal cells
0	–	100%	–	100%
10	1%	99%	3%	97%
40	11%	89%	16%	84%
90	15%	85%	24%	76%
180	20%	80%	30%	70%
300	26%	74%	40%	60%

the mean cell wall thickness from 0.037 ± 0.005 μm to 0.026 ± 0.004 μm at 300 min. Relative to the control group, geraniol induced progressive thinning of the cell wall, consistent with marked impairment of envelope integrity. Collectively, these results suggest that geraniol severely disrupts the ultrastructural organization of *S. aureus* and promotes progressive deterioration of the bacterial envelope.

Molecular dynamics analysis of geraniol interactions with the cell membrane

To explore the mechanism by which geraniol disrupts bacterial membranes, molecular dynamics simulations were performed using a model lipid bilayer. The simulations predicted rapid penetration of geraniol into the membrane interface within 1 ns, with strong interactions between its hydroxyl group and the hydrophobic tails of the membrane lipids (Figure 8). Following initial insertion, geraniol remained predominantly within the outer leaflet and subsequently migrated toward the bilayer interior, where it persisted for the remainder of the simulation. This behavior induced localized disorder within the lipid matrix and disrupted bilayer organization, indicating substantial perturbation of membrane architecture. These predictions suggest that geraniol directly interacts with the cell membrane, destabilizes lipid bilayer organization, and alters membrane structure.

Geraniol-induced release of cellular constituents

Extracellular and intracellular levels of nucleic acids and proteins were measured to assess membrane-associated

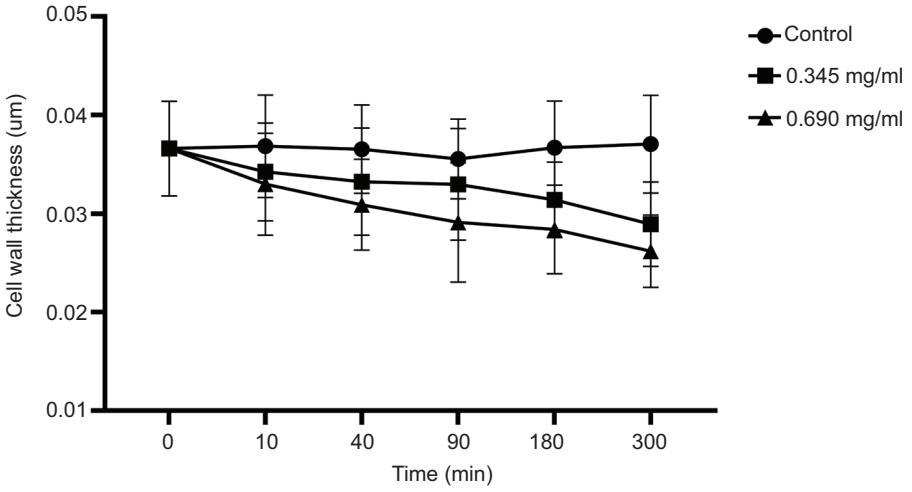

Figure 7. Effects of geraniol on cell wall thickness of *S. aureus*. At least 50 cells were analyzed at each time point. Error bars represent SD.

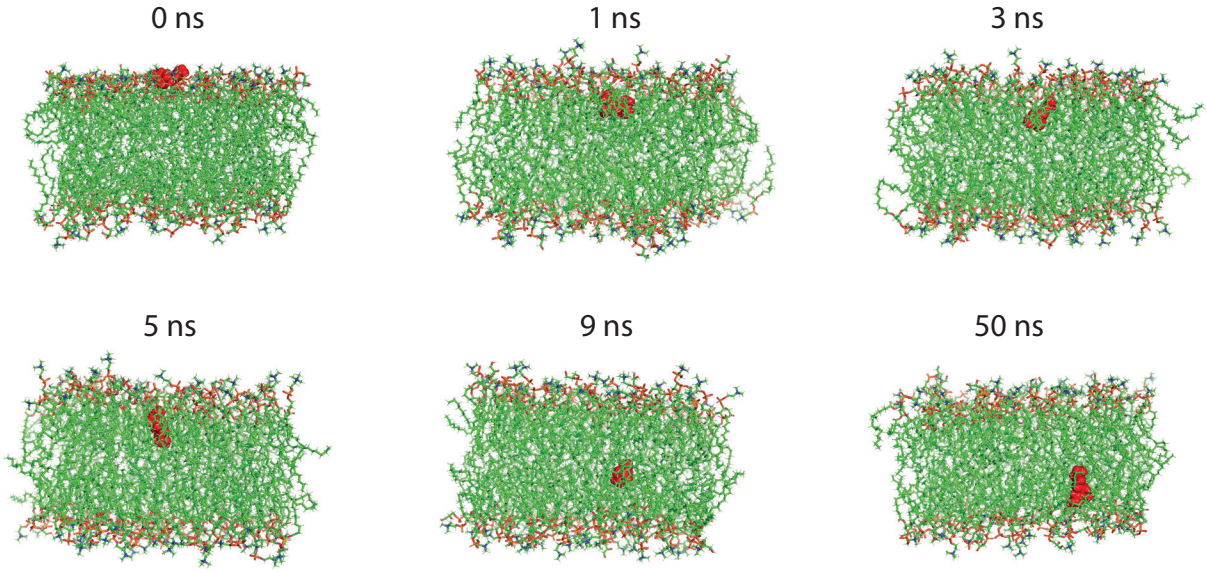

Figure 8. Representative molecular dynamics snapshots of interaction between geraniol and cell membrane, showing initial state, membrane penetration, and equilibrium state from left to right.

leakage after geraniol exposure. As shown in Figures 9A, 9C, and 9E, exposure to 1.380 mg/mL geraniol for 6 h increased extracellular DNA and RNA levels by 164.94 ng/mL and 132.81 ng/mL, respectively, while extracellular protein content reached a level 15.92-fold higher than that of the control group. In parallel, intracellular DNA, RNA, and protein contents were significantly reduced after treatment (Figures 9B, 9D, and 9F). These findings indicate that geraniol exposure promotes substantial leakage of nucleic acids and proteins from *S. aureus* cells.

Effects of geraniol on cell membrane integrity

The impact of geraniol on membrane integrity in *S. aureus* was evaluated using a Live/Dead Bacterial Viability Kit combined with flow cytometry (Witkowska *et al.*, 2013). Density plots separated cells into two regions: R1, representing dead cells or those with compromised membrane integrity, and R2, representing live cells or those with intact cell membranes. As demonstrated in Figure 10A, the negative control contained 99.10% live cells, with only 0.44% exhibiting membrane damage. In

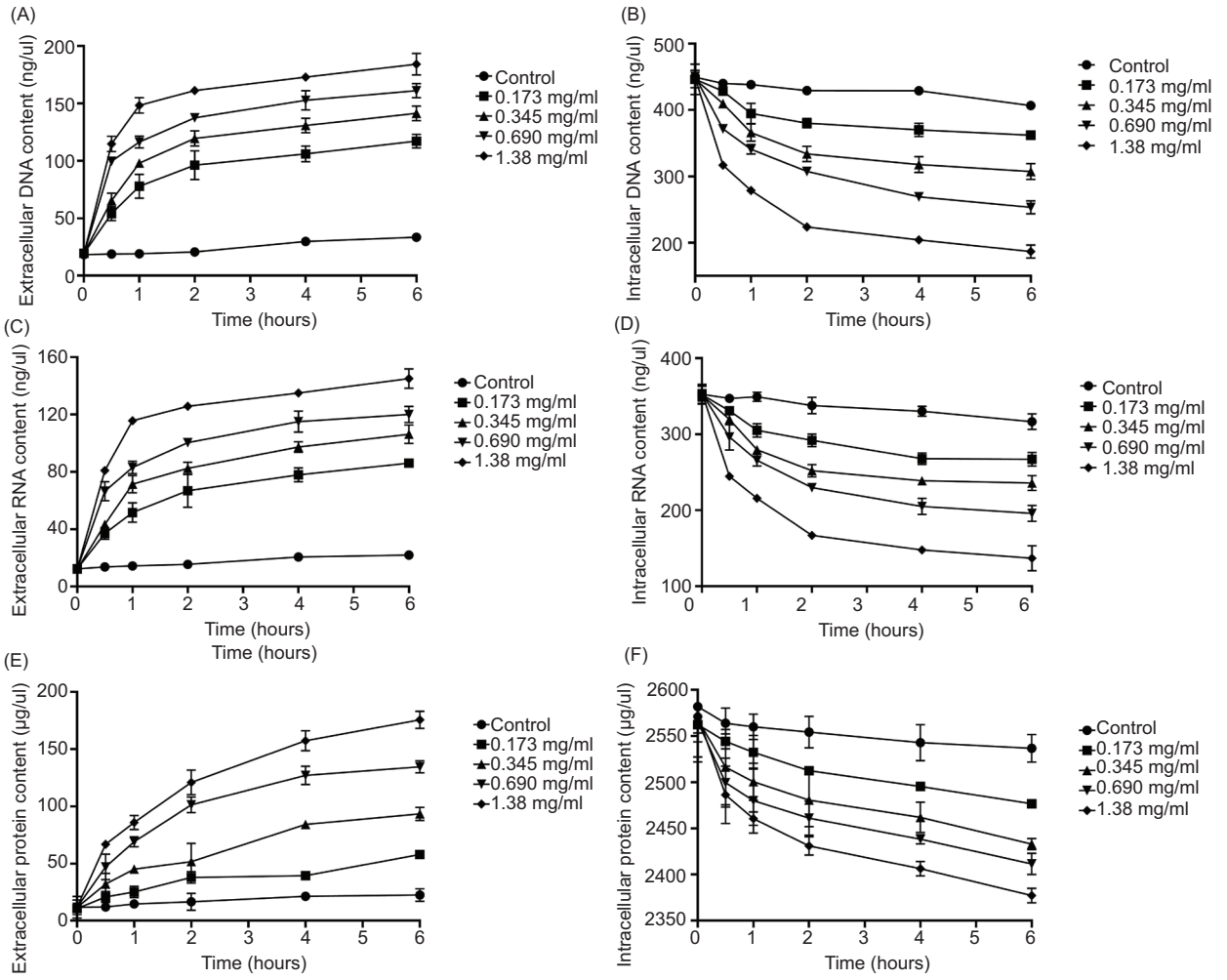

Figure 9. Release of cellular constituents following geraniol treatment. Extracellular DNA (A), intracellular DNA (B), extracellular RNA (C), intracellular RNA (D), extracellular protein (E), and intracellular protein (F). Values are presented as means ± SD (error bars) from three independent experiments.

contrast, in the positive control group treated with 70% isopropyl alcohol, 96.70% of cells exhibited compromised membrane integrity, and only 0.67% remained viable (Figure 10B). As shown in Figure 10C–F, geraniol induced a concentration-dependent decline in the proportion of live cells, from 91.52% at 0.173 mg/mL to 20.22% at 1.380 mg/mL, accompanied by an increase in membrane-compromised cells from 7.25% to 81.95%. These findings indicate that geraniol disrupts membrane integrity in *S. aureus* cells in a concentration-dependent manner.

Effects of geraniol on membrane fluidity

Membrane fluidity in *S. aureus* following geraniol treatment was assessed using the hydrophobic fluorescent probe DPH to evaluate changes in the cytoplasmic membrane. Because DPH fluorescence polarization is inversely associated with membrane fluidity, lower polarization values indicate a more fluid membrane state (He, 2023). Geraniol treatment altered membrane biophysical properties, with fluorescence polarization decreasing from 0.410 to 0.380 as the concentration increased from 0.173 mg/mL to 1.380 mg/mL (Figure 11), indicating a significant increase in membrane fluidity ($p \leq 0.0001$).

Effects of geraniol on membrane proteins

As variation in phenylalanine fluorescence can reflect interactions between antibacterial agents and membrane proteins (Wang *et al.*, 2017), fluorescence signals from phenylalanine residues were monitored to evaluate the effects of geraniol on membrane proteins. As shown in Figure 12, geraniol induced progressive quenching

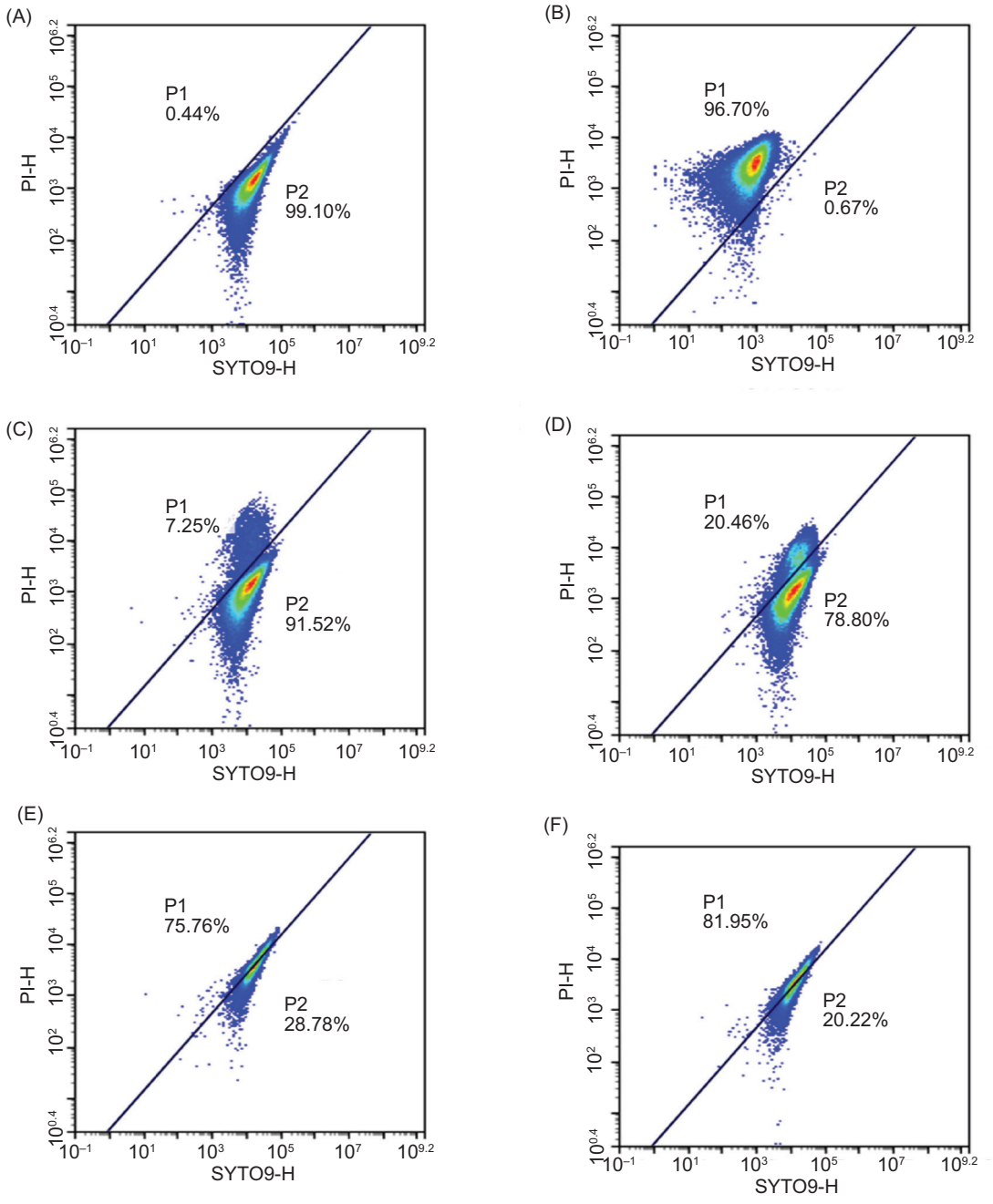

Figure 10. Flow cytometric analysis of SYTO9/PI-stained *S. aureus*. Untreated cells (A), cells treated with 70% isopropyl alcohol for 30 min (B), cells treated with 0.173 mg/mL geraniol for 30 min (C), cells treated with 0.345 mg/mL geraniol for 30 min (D), cells treated with 0.690 mg/mL geraniol for 30 min (E), and cells treated with 1.380 mg/mL geraniol for 30 min (F). Regions R1 and R2 represent membrane-damaged or dead cells and live cells, respectively.

of phenylalanine fluorescence in a concentration-dependent manner, indicating an interaction with membrane proteins.

Discussion

Although geraniol has been reported to possess antibacterial activity against *S. aureus*, the sequence of cellular events leading to bacterial death and the causal relationship between membrane damage and downstream structural alterations remain poorly defined (Albano *et al.*, 2016; Lertsatitthanakorn *et al.*, 2010). In particular, it is unclear whether membrane disruption serves as an initiating event or a secondary consequence of general cellular deterioration. This study applied a time-resolved analytical framework to investigate the dynamic

progression of morphological, biophysical, and ultrastructural changes in *S. aureus* following geraniol exposure, with the aim of clarifying the temporal order of key damaging events.

Antibacterial activity of geraniol

The MIC and MBC of geraniol against MRSA ATCC 43300 were determined to be 0.690 mg/mL and 1.380 mg/mL, respectively. These values are similar to those reported by Castro *et al*., (2025) and Aiemsaard *et al*., (2011) across multiple *S. aureus* strains, indicating reproducible antibacterial activity. Growth curve and time-kill assays further demonstrated that geraniol at concentrations ≥ 0.518 mg/mL completely suppressed bacterial proliferation, and at 1.380 mg/mL reduced viable counts by > 5 $\log_{10}$ CFU/mL within 2 h, confirming rapid bactericidal action.

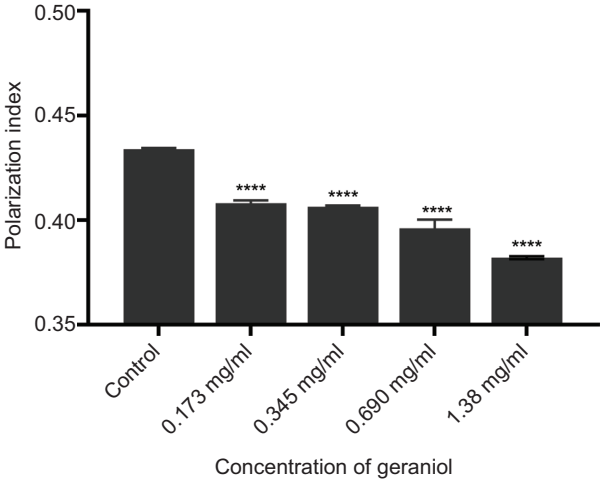

Figure 11. Effects of geraniol on membrane fluidity of *S. aureus*. Values are presented as means ± SD from three independent experiments. **p* ≤ 0.05, ***p* ≤ 0.01, ****p* ≤ 0.001, and *****p* ≤ 0.0001.

Temporal evidence of membrane damage, structural alterations and barrier dysfunction

Electron microscopy (SEM, TEM, and SR-SIM) revealed that geraniol induced surface shrinkage and separation of the cell membrane from the cell wall within 10 min of exposure. In contrast, significant cell wall thinning and DNA condensation occurred at later time points (40–300 min). This temporal ordering suggests that membrane injury precedes downstream structural damage rather than being a nonspecific consequence of cell death. To further test causality, future experiments using membrane stabilizers, for example, glycine betaine, could determine whether preserving membrane integrity concurrently attenuates subsequent wall thinning and DNA condensation (Wang *et al*., 2019).

Molecular dynamics simulations provided complementary evidence for direct membrane targeting. Geraniol inserted into the lipid bilayer within 1 ns and remained associated throughout the 50 ns simulation, inducing localized lipid disordering. This behavior is consistent with the experimentally observed increase in membrane fluidity with fluorescence polarization decreased from 0.410 to 0.380, and conformational changes in membrane proteins, as indicated by phenylalanine fluorescence quenching. Although the current simulation model lacks native membrane proteins, future studies incorporating representative targets, such as FtsZ or PBP2, may enhance physiological relevance (Chen *et al*., 2023; Knapp *et al*., 2024).

The functional consequences of membrane disruption were further quantified using flow cytometry and

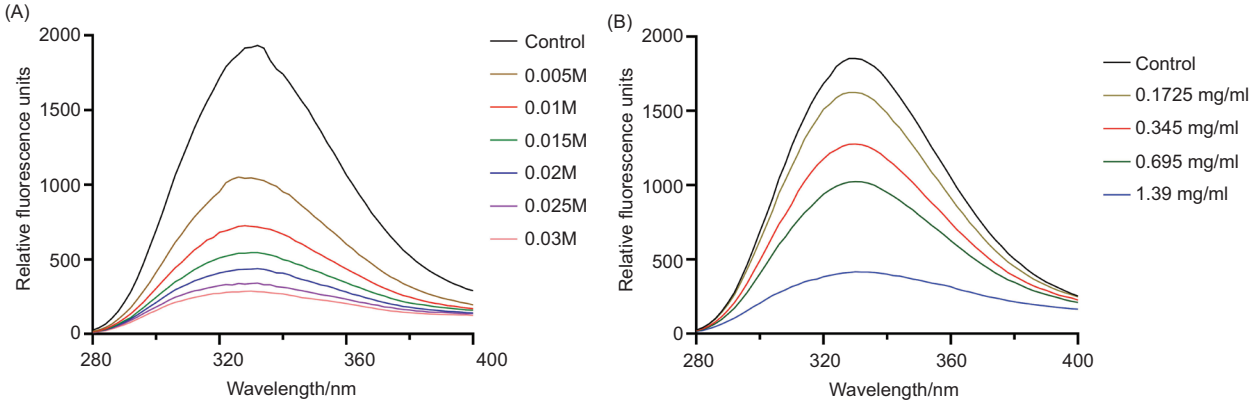

Figure 12. Fluorescence emission spectra of phenylalanine residues in membrane proteins of *S. aureus* following treatment with different concentrations of KI (A) or geraniol (B). λex = 258 nm.

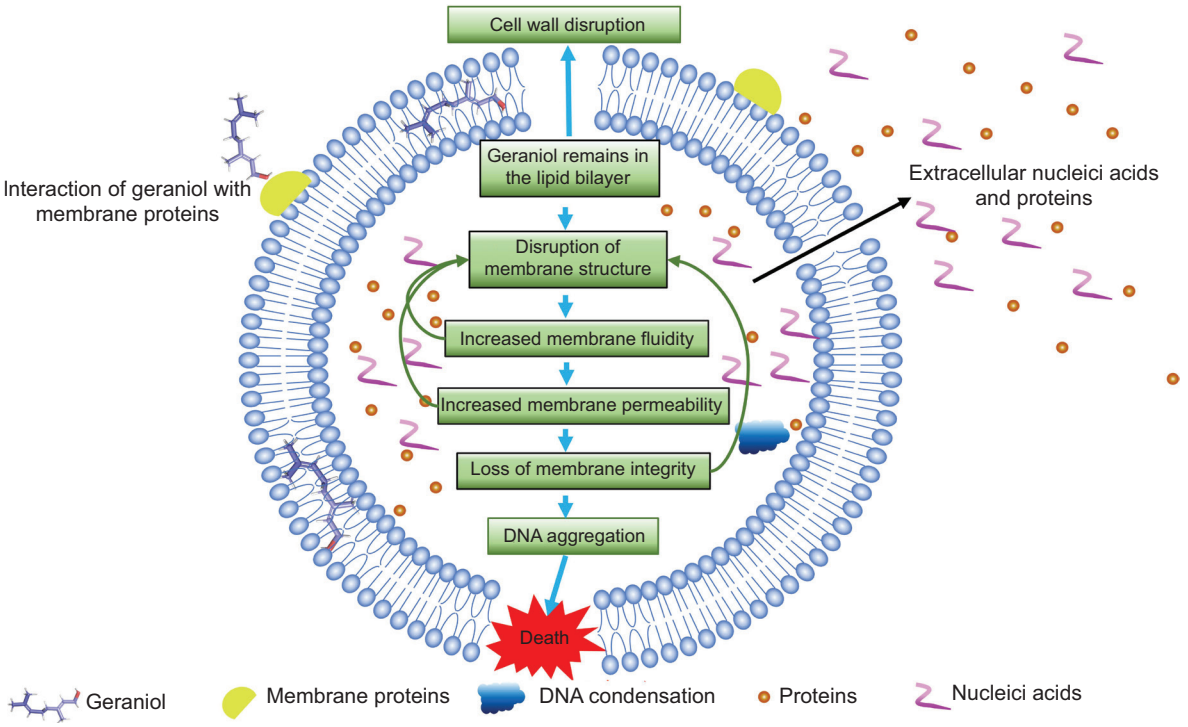

Figure 13. Schematic of the antibacterial mechanism of geraniol.

constituent leakage assays. Exposure to 1.380 mg/mL geraniol for 30 min resulted in 81.95% of cells displaying compromised membrane integrity, as determined by SYTO9/PI staining. Concomitantly, extracellular levels of DNA, RNA, and protein increased by 9.61-, 11.82-, and 15.92-fold, respectively, while their intracellular counterparts decreased correspondingly. These results collectively indicate that disruption of the membrane barrier function represents a dominant and quantifiable phenotype associated with geraniol action, similar to observations in other Gram-positive pathogens such as *Burkholderia cenocepacia* (Vasireddy *et al.*, 2018).

Cell wall thinning and DNA condensation might be downstream consequences

Geraniol treatment reduced mean cell wall thickness from 0.037 μm to 0.026 μm in a time- and concentration-dependent manner. This thinning is unlikely to be an independent event; rather, it may result from impaired cell wall synthesis secondary to membrane dysfunction. An intact membrane is essential for maintaining ion gradients, particularly Mg^{2+}, and ATP production. Mg^{2+} serves as a critical cofactor for peptidoglycan synthases, and ATP drives the synthesis and translocation of peptidoglycan precursors (Munshi *et al.*, 2013; Payandeh & Pai, 2006). It is therefore hypothesized that geraniol-induced membrane damage may cause Mg^{2+} leakage and energy depletion, which could in turn compromise cell wall integrity (Caillet *et al.*, 2005; Gill & Holley, 2006). Direct measurements of intracellular Mg^{2+} and ATP levels are needed to validate this hypothesis.

DNA condensation was observed as early as 10 min at 0.690 mg/mL geraniol, but only after 300 min at the sub-inhibitory concentration (0.345 mg/mL). This concentration-dependent delay suggests that DNA condensation is not a direct effect of geraniol but rather a secondary response to preceding membrane injury. Potential mechanisms include activation of nucleoid-associated proteins following ionic imbalance or induction of the SOS stress response under energy crisis (Castro *et al.*, 2025; Natriashvili *et al.*, 2025). Future studies employing SOS reporter strains and ATP quantification may help distinguish among these possibilities.

Translational potential and study limitations

Geraniol is FDA-approved as a food additive and exhibits a favorable safety profile (Ben Ammar, 2023; CHO *et al.*, 2016; Lei *et al.*, 2019; Mączka *et al.*, 2020; Rizzello *et al.*, 2018). However, its strong odor at higher concentrations may limit direct application in

food preservation. Future strategies, such as structural modification (e.g., esterification) or nanoencapsulation (e.g., cyclodextrin inclusion or liposomal formulations), could reduce the effective concentration and mitigate sensory off-effects. Recent studies by De Paula Santos *et al*., (2025) and Silva Pontes *et al*., (2023) have shown that nanoencapsulation enhances the antibacterial efficacy of geraniol while reducing toxicity, providing a viable path forward.

Several limitations of this study should be acknowledged. The primary experiments were conducted using a single reference strain (ATCC 43300); therefore, the generalizability of the proposed mechanism to diverse clinical MRSA isolates requires further validation. In addition, the molecular dynamics simulations employed a simplified lipid bilayer model without native membrane proteins, which may not fully recapitulate the native bacterial membrane environment (Freeman *et al*., 2024; Joodaki *et al*., 2022). Moreover, the proposed links between membrane injury, cell wall thinning, and DNA condensation remain largely correlative. Targeted experiments, including membrane stabilizer intervention, direct measurement of Mg^{2+} and ATP levels, and photoaffinity labeling-based proteomics, are warranted to establish definitive causality (Iqbal *et al*., 2021; Tian *et al*., 2008; Zhu, 2023).

Conclusions

In summary, this study proposes a cascade model in which geraniol-induced membrane damage serves as the primary initiating event, followed by secondary cell wall thinning and DNA condensation in *S. aureus*. While direct causal validation is still needed, the integrated functional, structural, biophysical, and computational evidence consistently supports the bacterial cell membrane as the principal target of geraniol. This mechanistic framework provides a theoretical basis for the further development of geraniol as a membrane-targeting antibacterial agent for food preservation and therapeutic applications.

Data Availability Statement

All data are available in this manuscript.

Mandatory Disclosure on Use of Artificial Intelligence

The authors declare the use of DeepSeek3.2 for language refinement. All references have been manually verified for accuracy and relevance.

Author Contributions

Fenghui Sun conceived and designed the project. Keshan Lin, Jialin Dai, and Rui Zhang performed the experiments and drafted the manuscript. Renkun Lai, Peng Zhang, Lizhu Shen, Lin Lin, and Chunyang Li analyzed the data. Fenghui Sun and Min Dai modified the manuscript. All authors discussed the results and approved the final manuscript.

Conflicts of Interest

The authors declare no conflicts of interest.

Funding

This study was supported by the National Natural Science Foundation of China (32270449, 82102442, 82472328), CMC Excellent-talent Program (2024yxGzn06), Sichuan Science and Technology Program (2025YFHZ0215, 2024YFFK0090), Open Fund of Aging Mechanisms and Interventions Key Laboratory of Sichuan Province (24LHFYSZ1-36, 25AMIKLSP05), Open Fund of Sichuan Provincial Engineering Laboratory for Prevention and Control Technology of Veterinary Drug Residue in Animal-origin (23LHNBZZD01), National Training Program of Innovation and Entrepreneurship for Undergraduates (202313705030), and Special Research Project of Sichuan Provincial Administration of Traditional Chinese Medicine (25MSZX555).

References

Aiemsaard, J., Aiumlamai, S., Aromdee, C., Taweechaisupapong, S., & Khunkitti, W. (2011). The effect of lemongrass oil and its major components on clinical isolate mastitis pathogens and their mechanisms of action on *Staphylococcus aureus* DMST 4745. Research in Veterinary Science, 91, e31–e37. https://doi.org/10.1016/j.rvsc.2011.01.012

Albano, M., Alves, F.C.B., Andrade, B.F.M.T., Barbosa, L.N., Pereira, A.F.M., Cunha, M.D.L.R.D.S.D., Rall, V.L.M., & Fernandes Júnior, A. (2016). Antibacterial and anti-staphylococcal enterotoxin activities of phenolic compounds. Innovative Food Science & Emerging Technologies, 38, 83–90. https://doi.org/10.1016/j.ifset.2016.09.003

Bagheri, S., Salehi, I., Ramezani-Aliakbari, F., Kourosh-Arami, M., & Komaki, A. (2022). Neuroprotective effect of geraniol on neurological disorders: A review article. Molecular Biology Reports, 49, 10865–10874. https://doi.org/10.1007/s11033-022-07755-w

Bai, J., Wu, Y., Liu, X., Zhong, K., Huang, Y., & Gao, H. (2015). Antibacterial activity of shikimic acid from pine needles of *Cedrus deodara* against *Staphylococcus aureus* through damage to the cell membrane. International Journal of Molecular Sciences, 16, 27145–27155. https://doi.org/10.3390/ijms161126015

Ben Ammar, R. (2023). Potential effects of geraniol on cancer and inflammation-related diseases: A review of the recent research findings. Molecules, 28, 3669. https://doi.org/10.3390/molecules28093669

Caillet, S., Shareck, F., & Lacroix, M. (2005). Effect of gamma radiation and oregano essential oil on murein and ATP concentration of *Escherichia coli* O157:H7. Journal of Food Protection, 68, 2571–2579. https://doi.org/10.4315/0362-028X-68.12.2571

Castro, I.M. de, Antunes, C., Valentim, C.C., Spoladori, L.F. de A., Suzukawa, H.T., Correia, G.F., Silva-Rodrigues, G., Borges, P.H.G., Bartolomeu-Gonçalves, G., Silva, M.L., Bispo, M. de L.F., Machado, R.R.B., Nakamura, C.V., Nakazato, G., Pinge-Filho, P., Tavares, E.R., Yamauchi, L.M., & Yamada-Ogatta, S.F. (2025). Synergistic antibacterial interaction of geraniol and biogenic silver nanoparticles on methicillin-resistant *Staphylococcus aureus*. Plants (Basel), 14, 1059. https://doi.org/10.3390/plants14071059

Chen, Y.W., Kong, W.-P., & Wong, K.-Y. (2023). The structural integrity of the membrane-embedded bacterial division complex FtsQBL studied with molecular dynamics simulations. Computational and Structural Biotechnology Journal, 21, 2602–2612. https://doi.org/10.1016/j.csbj.2023.03.052

Cheung, G.Y.C., Bae, J.S., & Otto, M. (2021). Pathogenicity and virulence of *Staphylococcus aureus*. Virulence, 12, 547–569. https://doi.org/10.1080/21505594.2021.1878688

Cho, M., So, I., Chun, J.N., & Jeon, J.-H. (2016). The antitumor effects of geraniol: Modulation of cancer hallmark pathways (Review). International Journal of Oncology, 48, 1772–1782. https://doi.org/10.3892/ijo.2016.3427

Creighton, M.A., Zhu, W., van Krieken, F., Petteruti, R.A., Gao, H., & Hurt, R.H. (2016). Three-dimensional graphene-based microbarriers for controlling release and reactivity in colloidal liquid phases. ACS Nano, 10, 2268–2276. https://doi.org/10.1021/acsnano.5b06963

De Paula Santos, W., Tavares, L.P., Pontes, C.G., Risso, W.E., Toci, A.T., De Oliveira, J.L., Fraceto, L.F., & Bueno dos Reis Martinez, C. (2025). Assessing the impacts of nanoencapsulated geraniol on amphibians: A step toward sustainable pesticide alternatives? Comparative Biochemistry and Physiology Part C: Toxicology & Pharmacology, 296, 110231. https://doi.org/10.1016/j.cbpc.2025.110231

D'Souza, S.P., Chavannavar, S.V., Kanchanashri, B., & Niveditha, S.B. (2017). Pharmaceutical perspectives of spices and condiments as alternative antimicrobial remedy. Journal of Evidence-Based Complementary & Alternative Medicine, 22, 1002–1010. https://doi.org/10.1177/2156587217703214

Ekhtelat, M., Khalili Borujeni, F., Siahpoosh, A., & Ameri, A. (2020). Chemical composition and antibacterial effects of some essential oils individually and in combination with sodium benzoate against methicillin-resistant *Staphylococcus aureus* and *Yersinia enterocolitica*. Veterinary Research Forum, 11, 333–338. https://doi.org/10.30466/vrf.2018.93152.2248

El Azab, E.F., Elguindy, N.M., Yacout, G.A., & Elgamal, D.A. (2020). Hepatoprotective impact of geraniol against CCl_4-induced liver fibrosis in rats. Pakistan Journal of Biological Sciences, 23, 1650–1658. https://doi.org/10.3923/pjbs.2020.1650.1658

Feng, X., Feng, K., Zheng, Q., Tan, W., Zhong, W., Liao, C., Liu, Y., Li, S., & Hu, W. (2022). Preparation and characterization of geraniol nanoemulsions and its antibacterial activity. Frontiers in Microbiology, 13, 1080300. https://doi.org/10.3389/fmicb.2022.1080300

Freeman, C.D., Hansen, T., Urbauer, R., Wilkinson, B.J., Singh, V.K., & Hines, K.M. (2024). Defective pgsA contributes to increased membrane fluidity and cell wall thickening in *Staphylococcus aureus* with high-level daptomycin resistance. mSphere, 9, e00115–24. https://doi.org/10.1128/msphere.00115-24

Friedman, M., Henika, P.R., & Mandrell, R.E. (2002). Bactericidal activities of plant essential oils and some of their isolated constituents against *Campylobacter jejuni*, *Escherichia coli*, *Listeria monocytogenes*, and *Salmonella enterica*. Journal of Food Protection, 65, 1545–1560. https://doi.org/10.4315/0362-028x-65.10.1545

Gill, A.O., & Holley, R.A. (2006). Disruption of *Escherichia coli*, *Listeria monocytogenes*, and *Lactobacillus sakei* cellular membranes by plant oil aromatics. International Journal of Food Microbiology, 108, 1–9. https://doi.org/10.1016/j.ijfoodmicro.2005.10.009

Gu, K., Ouyang, P., Hong, Y., Dai, Y., Tang, T., He, C., Shu, G., Liang, X., Tang, H., Zhu, L., Xu, Z., & Yin, L. (2022). Geraniol inhibits biofilm formation of methicillin-resistant *Staphylococcus aureus* and increases the therapeutic effect of vancomycin in vivo. Frontiers in Microbiology, 13, 960728. https://doi.org/10.3389/fmicb.2022.960728

Guimarães, A.C., Meireles, L.M., Lemos, M.F., Guimarães, M.C.C., Endringer, D.C., Fronza, M., & Scherer, R. (2019). Antibacterial activity of terpenes and terpenoids present in essential oils. Molecules, 24, 2471. https://doi.org/10.3390/molecules24132471

Hatlen, T.J., & Miller, L.G. (2021). Staphylococcal skin and soft tissue infections. Infectious Disease Clinics of North America, 35, 81–105. https://doi.org/10.1016/j.idc.2020.10.003

He, W. (2023). DPH probe method for liposome-membrane fluidity determination. Methods in Molecular Biology, 2622, 241–244. https://doi.org/10.1007/978-1-0716-2954-3_21

Hess, B., Kutzner, C., Van der Spoel, D., & Lindahl, E. (2008). GROMACS 4: Algorithms for highly efficient, load-balanced, and scalable molecular simulation. Journal of Chemical Theory and Computation, 4, 435–447. https://doi.org/10.1021/ct700301q

Hou, X., Li, J., Tang, H., Li, Q., Shen, G., Li, S., Chen, A., Peng, Z., Zhang, Y., Li, C., & Zhang, Z. (2022). Antibacterial peptide NP-6 affects *Staphylococcus aureus* by multiple modes of action. International Journal of Molecular Sciences, 23, 7812. https://doi.org/10.3390/ijms23147812

Huo, G., Li, X., Abubaker, M.A., Liang, T., Zhang, J., & Chen, X. (2022). A composition analysis and an antibacterial activity mechanism exploration of essential oil obtained from *Artemisia giraldii* Pamp. Molecules, 27, 7300. https://doi.org/10.3390/molecules27217300

Iqbal, D., Khan, M.S., Waiz, M., Rehman, M.T., Alaidarous, M., Jamal, A., Alothaim, A.S., AlAjmi, M.F., Alshehri, B.M., Banawas, S., Alsaweed, M., Madkhali, Y., Algarni, A., Alsagaby, S.A., & Alturaiki, W. (2021). Exploring the binding pattern of geraniol with

acetylcholinesterase through in silico docking, molecular dynamics simulation, and in vitro enzyme inhibition kinetics studies. Cells, 10, 3533. https://doi.org/10.3390/cells10123533

Jayachandran, M., Chandrasekaran, B., & Namasivayam, N. (2015). Geraniol attenuates fibrosis and exerts anti-inflammatory effects on diet-induced atherogenesis by the NF-κB signaling pathway. European Journal of Pharmacology, 762, 102–111. https://doi.org/10.1016/j.ejphar.2015.05.039

Jensen, C., Li, H., Vestergaard, M., Dalsgaard, A., Frees, D., & Leisner, J.J. (2020). Nisin damages the septal membrane and triggers DNA condensation in methicillin-resistant *Staphylococcus aureus*. Frontiers in Microbiology, 11, 1007. https://doi.org/10.3389/fmicb.2020.01007

Joodaki, F., Martin, L.M., & Greenfield, M.L. (2022). Generation and computational characterization of a complex *Staphylococcus aureus* lipid bilayer. Langmuir, 38, 9481–9499. https://doi.org/10.1021/acs.langmuir.2c00483

Kannappan, A., Balasubramaniam, B., Ranjitha, R., Srinivasan, R., Packiavathy, I.A.S.V., Balamurugan, K., Pandian, S.K., & Ravi, A.V. (2019). In vitro and in vivo biofilm inhibitory efficacy of geraniol–cefotaxime combination against *Staphylococcus* spp. Food and Chemical Toxicology, 125, 322–332. https://doi.org/10.1016/j.fct.2019.01.008

Kim, C.-M., Ko, Y.J., Lee, S.-B., & Jang, S.J. (2022). Adjuvant antimicrobial activity and resensitization efficacy of geraniol in combination with antibiotics on *Acinetobacter baumannii* clinical isolates. PLoS ONE, 17, e0271516. https://doi.org/10.1371/journal.pone.0271516

Kim, W., Zhu, W., Hendricks, G.L., Van Tyne, D., Steele, A.D., Keohane, C.E., Fricke, N., Conery, A.L., Shen, S., Pan, W., Lee, K., Rajamuthiah, R., Fuchs, B.B., Vlahovska, P.M., Wuest, W.M., Gilmore, M.S., Gao, H., Ausubel, F.M., & Mylonakis, E. (2018). A new class of synthetic retinoid antibiotics effective against bacterial persisters. Nature, 556, 103–107. https://doi.org/10.1038/nature26157

Kim, W., Zou, G., Pan, W., Fricke, N., Faizi, H.A., Kim, S.M., Khader, R., Li, S., Lee, K., Escorba, I., Vlahovska, P.M., Gao, H., Ausubel, F.M., & Mylonakis, E. (2020). The neutrally charged diarylurea compound PQ401 kills antibiotic-resistant and antibiotic-tolerant *Staphylococcus aureus*. mBio, 11. https://doi.org/10.1128/mBio.01140-20

Knapp, B.D., Shi, H., & Huang, K.C. (2024). Complex state transitions of the bacterial cell division protein FtsZ. Molecular Biology of the Cell, 35, ar130. https://doi.org/10.1091/mbc.E23-11-0446

Lei, Y., Fu, P., Jun, X., & Cheng, P. (2019). Pharmacological properties of geraniol: A review. Planta Medica, 85, 48–55. https://doi.org/10.1055/a-0750-6907

Lertsatitthanakorn, P., Taweechaisupapong, S., Arunyanart, C., Aromdee, C., & Khunkitti, W. (2010). Effect of citronella oil on time-kill profile, leakage, and morphological changes of *Propionibacterium acnes*. Journal of Essential Oil Research, 22, 270–274. https://doi.org/10.1080/10412905.2010.9700322

Li, W.-R., Zeng, T.-H., Zhang, Z.-Q., Shi, Q.-S., & Xie, X.-B. (2023). Geraniol attenuates virulence factors by inhibiting quorum sensing of *Pseudomonas aeruginosa*. Frontiers in Microbiology, 14, 1190619. https://doi.org/10.3389/fmicb.2023.1190619

Mączka, W., Wińska, K., & Grabarczyk, M. (2020). One hundred faces of geraniol. Molecules, 25, 3303. https://doi.org/10.3390/molecules25143303

Mamur, S., Yüzbaşıoğlu, D., Ünal, F., & Aksoy, H. (2012). Genotoxicity of food preservative sodium sorbate in human lymphocytes in vitro. Cytotechnology, 64, 553–562. https://doi.org/10.1007/s10616-012-9434-5

Mele, T., & Madrenas, J. (2010). TLR2 signalling: At the crossroads of commensalism, invasive infections and toxic shock syndrome by *Staphylococcus aureus*. International Journal of Biochemistry & Cell Biology, 42, 1066–1071. https://doi.org/10.1016/j.biocel.2010.03.021

Munshi, T., Gupta, A., Evangelopoulos, D., Guzman, J.D., Gibbons, S., Keep, N.H., & Bhakta, S. (2013). Characterisation of ATP-dependent Mur ligases involved in the biogenesis of cell wall peptidoglycan in *Mycobacterium tuberculosis*. PLoS ONE, 8, e60143. https://doi.org/10.1371/journal.pone.0060143

Murbach Teles Andrade, B.F., Nunes Barbosa, L., Bérgamo Alves, F.C., Albano, M., Mores Rall, V.L., Sforcin, J.M., Fernandes, A.A.H., & Fernandes Júnior, A. (2016). The antibacterial effects of *Melaleuca alternifolia*, *Pelargonium graveolens*, and *Cymbopogon martinii* essential oils and major compounds on liquid and vapor phases. Journal of Essential Oil Research, 28, 227–233. https://doi.org/10.1080/10412905.2015.1099571

Natriashvili, A., Mohammadsadeghi, N., Smudde, E., Berghoff, B., Ulbrich, M. H., & Koch, H. G. (2025). The small bacterial membrane protein YohP induces nucleoid condensation in E. coli and inhibits oligomerization of antimicrobial peptides. MicroLife, 6, uqaf030. https://doi.org/10.1093/femsml/uqaf030

Ning, K., Zhou, R., & Li, M. (2023). Antimicrobial resistance and molecular typing of *Staphylococcus aureus* isolates from raw milk in Hunan Province. PeerJ, 11. https://doi.org/10.7717/peerj.15847

Novais, C., Molina, A.K., Abreu, R.M.V., Santo-Buelga, C., Ferreira, I.C.F.R., Pereira, C., & Barros, L. (2022). Natural food colorants and preservatives: A review, a demand, and a challenge. Journal of Agricultural and Food Chemistry, 70, 2789–2805. https://doi.org/10.1021/acs.jafc.1c07533

Nunes Nascimento, J.C., Alvarenga, V.O., Paulino, B.N., de Cerqueira e Silva, A.B., Matos, J.R., Rosário, I.L.D.S., Andrade, I.H.P., Silva, J.G., & Costa, M. (2025). *Staphylococcus aureus* in food safety: Antimicrobial resistance, detection technologies, and future perspectives. Critical Reviews in Food Science and Nutrition, 1–24. https://doi.org/10.1080/10408398.2025.2528165

Olszewska, M.A., Gędas, A., & Simões, M. (2020). The effects of eugenol, trans-cinnamaldehyde, citronellol, and terpineol on *Escherichia coli* biofilm control as assessed by culture-dependent and -independent methods. Molecules, 25, 2641. https://doi.org/10.3390/molecules25112641

Pavan, B., Dalpiaz, A., Marani, L., Beggiato, S., Ferraro, L., Canistro, D., Paolini, M., Vivarelli, F., Valerii, M.C., Comparone, A., De Fazio, L., & Spisni, E. (2018). Geraniol

pharmacokinetics, bioavailability, and its multiple effects on liver antioxidant and xenobiotic-metabolizing enzymes. Frontiers in Pharmacology, 9, 18. https://doi.org/10.3389/fphar.2018.00018

Payandeh, J., & Pai, E.F. (2006). A structural basis for Mg^{2+} homeostasis and the CorA translocation cycle. The EMBO Journal, 25, 3762–3773. https://doi.org/10.1038/sj.emboj.760126

Ribeiro-Santos, R., Andrade, M., Melo, N.R. de, & Sanches-Silva, A. (2017). Use of essential oils in active food packaging: Recent advances and future trends. Trends in Food Science & Technology, 61, 132–140. https://doi.org/10.1016/j.tifs.2016.11.021

Rizzello, F., Ricci, C., Scandella, M., Cavazza, E., Giovanardi, E., Valerii, M.C., Campieri, M., Comparone, A., De Fazio, L., Candela, M., Turroni, S., & Spisni, E. (2018). Dietary geraniol ameliorates intestinal dysbiosis and relieves symptoms in irritable bowel syndrome patients: A pilot study. BMC Complementary and Alternative Medicine, 18, 338. https://doi.org/10.1186/s12906-018-2403-6

Royce, L.A., Liu, P., Stebbins, M.J., Hanson, B.C., & Jarboe, L.R. (2013). The damaging effects of short-chain fatty acids on *Escherichia coli* membranes. Applied Microbiology and Biotechnology, 97, 8317–8327. https://doi.org/10.1007/s00253-013-5113-5

Scallan, E., Hoekstra, R.M., Angulo, F.J., Tauxe, R.V., Widdowson, M.-A., Roy, S.L., Jones, J.L., & Griffin, P.M. (2011). Foodborne illness acquired in the United States—major pathogens. Emerging Infectious Diseases, 17, 7–15. https://doi.org/10.3201/eid1701.P11101

Selim, S., Almuhayawi, M.S., Alruhaili, M.H., Zakai, S.A., & Warrad, M. (2022). Generating new mixtures of food additives with antimicrobial and cytotoxic potency against *Bacillus cereus* and *Staphylococcus aureus*. Food Science & Nutrition, 10, 470–476. https://doi.org/10.1002/fsn3.2691

Shi, C., Che, M., Zhang, X., Liu, Z., Meng, R., Bu, X., Ye, H., & Guo, N. (2018). Antibacterial activity and mode of action of totarol against *Staphylococcus aureus* in carrot juice. Journal of Food Science and Technology, 55, 924–934. https://doi.org/10.1007/s13197-017-3000-2

Silva, G.D.S.E., Marques, J.N. de J., Linhares, E.P.M., Bonora, C.M., Costa, É.T., & Saraiva, M.F. (2022). Review of anticancer activity of monoterpenoids: Geraniol, nerol, geranial, and neral. Chemico-Biological Interactions, 362, 109994. https://doi.org/10.1016/j.cbi.2022.109994

Silva Pontes, C., Garcia de Carvalho, G., Rosa Perin Leite, A., Chorilli, M., & Palomari Spolidorio, D.M. (2023). Improving drug delivery on *Candida albicans* using geraniol nanoemulsion. Pharmaceutics, 15, 2475. https://doi.org/10.3390/pharmaceutics15102475

Singh, G., & Katoch, M. (2020). Antimicrobial activities and mechanism of action of *Cymbopogon khasianus* (Munro ex Hackel) Bor essential oil. BMC Complementary Medicine and Therapies, 20, 331. https://doi.org/10.1186/s12906-020-03112-1

Song, M., Sun, J., Lv, K., Li, J., Shi, J., & Xu, Y. (2025). A comprehensive review of pathology and treatment of *Staphylococcus aureus* osteomyelitis. Clinical and Experimental Medicine, 25, 131. https://doi.org/10.1007/s10238-025-01595-1

Song, X., Liu, T., Wang, L., Liu, L., Li, X., & Wu, X. (2020). Antibacterial effects and mechanism of mandarin (*Citrus reticulata* L.) essential oil against *Staphylococcus aureus*. Molecules, 25, 4956. https://doi.org/10.3390/molecules25214956

Sun, F., Long, N., Wang, X., Lin, L., Li, J., Wu, X., Luo, Y., & Dai, M. (2018). In vitro antibacterial activity of geraniol against methicillin-resistant *Staphylococcus aureus*. Chinese Journal of Antibiotics, 43, 921–926. https://doi.org/10.13461/j.cnki.cja.005963

Tabah, A., & Laupland, K.B. (2022). Update on *Staphylococcus aureus* bacteraemia. Current Opinion in Critical Care, 28, 495–504. https://doi.org/10.1097/MCC.0000000000000974

Teshome, E., Forsido, S.F., Rupasinghe, H.P.V., & Olika Keyata, E. (2022). Potentials of natural preservatives to enhance food safety and shelf life: A review. The Scientific World Journal, 2022, 9901018. https://doi.org/10.1155/2022/9901018

Tian, R., Li, L., Tang, W., Liu, H., Ye, M., Zhao, Z.K., & Zou, H. (2008). Chemical proteomic study of isoprenoid chain interactome with a synthetic photoaffinity probe.

Vasireddy, L., Bingle, L.E.H., & Davies, M.S. (2018). Antimicrobial activity of essential oils against multidrug-resistant clinical isolates of the *Burkholderia cepacia* complex. PLoS ONE, 13, e0201835. https://doi.org/10.1371/journal.pone.0201835

Wang, J., Ma, X., Li, J., Shi, L., Liu, L., Hou, X., Jiang, S., Li, P., Lv, J., Han, L., Cheng, Y., & Han, B. (2023). The synergistic antimicrobial effect and mechanism of nisin and oxacillin against methicillin-resistant *Staphylococcus aureus*. International Journal of Molecular Sciences, 24, 6697. https://doi.org/10.3390/ijms24076697

Wang, L., Bokhary, S.U.F., Xie, B., Hu, S., Jin, P., & Zheng, Y. (2019). Biochemical and molecular effects of glycine betaine treatment on membrane fatty acid metabolism in cold-stored peaches. Postharvest Biology and Technology, 154, 58–69. https://doi.org/10.1016/j.postharvbio.2019.04.007

Wang, L.-H., Wang, M.-S., Zeng, X.-A., Xu, X.-M., & Brennan, C.S. (2017). Membrane and genomic DNA dual-targeting of citrus flavonoid naringenin against *Staphylococcus aureus*. Integrative Biology, 9, 820–829. https://doi.org/10.1039/c7ib00095b

Wei, M., Yu, H., Guo, Y., Cheng, Y., Xie, Y., & Yao, W. (2021). Antibacterial activity of *Sapindus* saponins against microorganisms related to food hygiene and the synergistic action mode of Sapindoside A and B against *Micrococcus luteus* in vitro. Food Control, 130, 108337. https://doi.org/10.1016/j.foodcont.2021.108337

Witkowska, A.M., Hickey, D.K., Alonso-Gomez, M., & Wilkinson, M. (2013). Evaluation of antimicrobial activities of commercial herb and spice extracts against selected food-borne bacteria. Journal of Food Research, 2, 37. https://doi.org/10.5539/jfr.v2n4p37

Wu, X., Wang, J., Li, J., Su, Z., & Zha, J. (2025). Mechanistic study on the susceptibility of *Staphylococcus aureus* to common antimicrobial preservatives mediated by wall teichoic acids. Applied and Environmental Microbiology, 91, e01023-25. https://doi.org/10.1128/aem.01023-25

Wu, Y., Bai, J., Zhong, K., Huang, Y., Qi, H., Jiang, Y., & Gao, H. (2016). Antibacterial activity and membrane-disruptive

mechanism of 3-*p*-trans-coumaroyl-2-hydroxyquinic acid, a novel phenolic compound from pine needles of *Cedrus deodara*, against *Staphylococcus aureus*. Molecules, 21, 1084. https://doi.org/10.3390/molecules21081084

Yu, S., Zhou, Y., Feng, D., Jiang, Q., Li, T., Jiang, G., Zhou, Z., & Li, H. (2023). Whole genome sequence-based characterization of virulence and antimicrobial resistance gene profiles of *Staphylococcus aureus* isolated from food poisoning incidents in eastern China. Frontiers in Microbiology, 14, 1225472. https://doi.org/10.3389/fmicb.2023.1225472

Yuan, Z., Ouyang, P., Gu, K., Rehman, T., Zhang, T., Yin, Z., Fu, H., Lin, J., He, C., Shu, G., Liang, X., Yuan, Z., Song, X., Li, L., Zou, Y., & Yin, L. (2019). The antibacterial mechanism of oridonin against methicillin-resistant *Staphylococcus aureus* (MRSA). Pharmaceutical Biology, 57, 710–716. https://doi.org/10.1080/13880209.2019.1674342

Zhu, Y. (2023). Combining native mass spectrometry and lipidomics to uncover specific membrane protein–lipid interactions from natural lipid sources. Chemical Science, 14(32), 8570–8582. https://doi.org/10.1039/d3sc01482g

Supplementary

Table S1. Experimental specifications used in SR-SIM.

Laser	Type & Power	Beam splitter	Grating	Dyes
405 nm	HR Diode – 50mW	BP 420-480 + LP 750	23 µm	Hoechst
488 nm	HR Diode – 50mW	BP 495-575 + LP 750	28 µm	WGA
561 nm	HR Diode – 100mW	BP 570-650 + LP 750	34 µm	Nile Red